NATURAL PRODUCT CHEMISTRY BULLETIN
VOL. 1, NO. 1, MAY 2025

Article History :
Submitted : 11 May 2025
Revised : 31 May 2025
Accepted : 5 June 2025

Rapid Mixing Synthesis of Polyaniline as an Adsorbent for Cr(VI) Ions

Alti Nurjaibah, Nenden Fauziah*

Department of Chemistry, Faculty of Mathematics and Natural Sciences,University of Garut, Jl. Jati No. 42B, Tarogong Kaler, West Java, 44151, Indonesia

*Email: nendenfauziah@uniga.ac.id

Abstract

The study of variations in the concentration of ammonium persulfate (APS) in the synthesis of polyaniline (PANI) using the rapid mixing method aims to determine the best candidate for chromium metal ion adsorbents among the PANI produced by varying the APS concentration. The variations in the APS concentration used were 0.1 M, 0.3 M, 0.5 M, and 0.7 M. The synthesized material was characterized using Fourier-transform infrared (FTIR) and Raman spectroscopy, while particle morphology and size were assessed through scanning electron microscopy (SEM). The results confirmed that the PANI produced was in the form of Emeraldine Salt (ES), with PANI 0.7 M yielding the highest mass of 3.03 grams and exhibiting globular particles ranging from 75 to 106 nm and a significant chromium (VI) ion adsorption capacity of 14.22 mg/g. These findings indicate that synthesizing PANI at an APS concentration of 0.7 M is highly effective for creating nano-sized PANI with excellent adsorption properties. This material shows great potential for use in water treatment applications related to leather tanning and as a counter electrode in dye-sensitized solar cells, thereby highlighting the broader impact of the research.

***Keywords**: adsorbent, ammonium persulfate, chromium-metal ion, polyaniline, rapid mixing*

1. INTRODUCTION

The leather tanning industry of Sukaregang Garut leaves chromium ion waste of 12.27 mg/L per sample taken from liquid waste from waste reservoirs and 0.18 mg/L per sample taken from liquid waste that is thrown away into the Environment per day (Senania, A and Noviyanti, 2022). The maximum chromium content in the leather industry, by the Quality Standards for Liquid Waste from the Leather Tanning Industry, based on the Decree of the Minister of State for the Environment Number 51/MENLH/10/1995, is 2 mg/L (Kusumaatmadja, S., 1995). The liquid waste discharged from the Sukaregang leather tanning industry is below the quality standards stipulated in the Decree of the Minister of State for the Environment No. 51/MENLH/10/1995. However, the chromium content should be below 0.05 mg/L if the water is used as drinking water (Georgaki & Charalambous, 2023). Chromium water contamination, especially of Cr(VI), will damage human health, including reproductive effects, nephrotoxic

effects, hepatotoxic effects, gastrointestinal effects, hematological disorders, skin problems, respiratory problems, and kidney damage (Xie, 2024).

Water discharged into the environment after use from various industrial processes must have chromium levels below the safe threshold. One effective way to overcome this pollution is to use adsorbents that bind dangerous metal ions (Eskandari et al., 2020). The use of adsorbents to overcome pollution is also practical and economical. Some materials commonly used as adsorbents of chromium ions, especially Cr (VI), include various types of carbon materials (Liang et al., 2021), biomass (Hashem et al., 2024), metal oxides (Wang et al., 2020), and conductive polymers (Eskandari et al., 2020). The most interesting conductive polymer is PANI because PANI has a facile synthesis method with good chemical stability, electrocatalytic activity, redox and ion exchange properties, environmental stability, and tunable properties. (Fauziah et al., 2023).

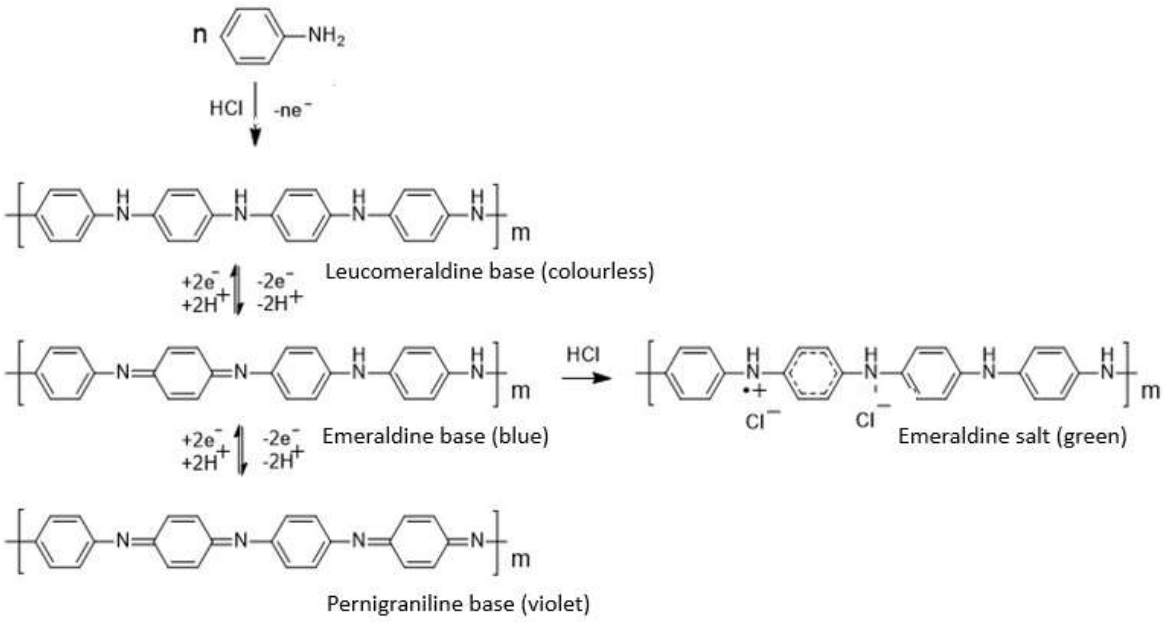

Figure 1. The structure and color of PANI with different oxidation levels.

PANI can interact with metal ions such as chromium. Thus, it has excellent potential as a chromium-adsorbing agent (Palimkar et al., 2023; Nurianingsih et al., 2019). PANI has three different oxidation states that are *leucomeradine* (fully reduced form), *emeraldine*(half-oxidized form), and *pernigraniline*(fully oxidized form) (Goswami et al., 2023). The difference in the color of the synthesized PANI can identify the success of PANI synthesis with a certain oxidation level. PANI *leucomeraldine base* is colorless, *emeraldine salt* is green, *emeraldine base* is blue, and *pernigraniline base* is violet, as seen in Figure 1 (Stejskal et al., 1996).

p-ISSN: XXXX-XXXX
e-ISSN: XXXX-XXXX

Synthesis of PANI using a variety of methods, including the conventional method (Sunarya et al., 2020), the emulsion method (Reza et al., 2021), the electrodeposition method (Fauziah et al., 2023), and the rapid mixing method (Amalina et al., 2019). This rapid mixing method, with its straightforward procedure and use of a simple apparatus, produces bulk nanofibers (Zakaria et al., 2015). The variation in ammonium persulfate (APS) concentration leads to different morphological results for PANI, from nanofibers (diameter 80 - 110 nm) to granules of 20 – 70 nm (Reza et al., 2019). We predict this variation in APS concentration will affect the level of PANI oxidation and the particle size, which, in turn, are expected to influence the adsorption capacities. However, to date, no research has evaluated the effectiveness of PANI resulting from rapid mixing synthesis with varying APS concentrations as an adsorbent of Cr (VI) metal ions. This study, therefore, aims to fill this gap by synthesizing PANI using the rapid mixing method and various APS concentrations and evaluating its adsorption capacity towards Cr (VI) ions.

2. MATERIAL AND METHODS

2.1. Material

Aniline (99%) was purchased from Sigma-Aldrich. Hydrochloric acid (HCl 37%) and ammonium persulfate (APS) were purchased from Merck. Ethanol (95%) and acetone were purchased from CV. Eralika Mitra Persada. All reagents were analytical grade. All reagents were used without further purification except for aniline. We first carry out a distillation process before aniline is used in synthesis.

2.2 Synthesis of HCl-doped PANI

PANI was prepared using a rapid mixing method (Amalina et al., 2019). Two initial solutions were prepared: (1) 1.87 g of aniline was dissolved in 50 mL of 1 M HCl, sonicated for 5 min, and then left at 0℃ for 22 h, and (2) 1.141 g of APS was dissolved in 50 mL of distilled water to obtain 0.1 M APS and then left at 0℃ for one h. The aniline-HCl was then added dropwise with APS under 200 rpm; the mixture was mixed for one hour. The process was allowed to continue for 22 h at 0℃ to ensure that all aniline monomers had become PANI. The reaction mixture was then filtered, rinsed with 1 M HCl and acetone repeatedly, and dried in an oven at 60℃ for two hours. Then, the procedure is repeated using APS of 0.3 M, 0.5 M, and 0.7 M, with the same volume of solution with different APS masses, as shown in Table 1.

p-ISSN: XXXX-XXXX
e-ISSN: XXXX-XXXX

Table 1. Variation concentraion of APS

Concentration of APS (M)	Mass of APS (g)	Volume of solution (ml)
0.1	1.141	50
0.3	3.423	50
0.5	5.705	50
0.7	7.987	50

2.3 Characterization of PANI

The functional groups of PANI are verified with a Bruker Alpha FTIR spectrometer. The PANI samples were prepared in KBr pellets and stored in a silica gel desiccator for 2 hours. Raman spectra were carried out using a Bruker Senterra Raman spectrometer equipped with a 50× Olympus long-working-distance MPlan semi-apochromatic objective lens. All samples were prepared on a gold surface and excited using a 532 nm Nd-YAG diode-pumped solid-state (DPSS) laser with a laser power of 10 mW and an integration time of 40 s, the co-addition of 2 times. Electron Microscopy analysis was carried out using a Hitachi SU3500 Scanning Electron Microscope. The SEM analysis, performed with the gold sputtering coating, 10.0 kV applied voltage, 5.7–5.8 mm working distance, and SE (Secondary Electron) mode, was conducted with thoroughness and attention to detail, ensuring the comprehensiveness of our research.

2.4 Adsorption Capacity of PANI

The adsorption capacity measurement starts with the standard curve of AAS with variation concentrations of 0, 2, 5, 10 and 15 ppm. The adsorption study is done with a ratio of PANI sample and $K_2Cr_2O_7$ 50 ppm as 1: 100 (0.001 g of sample in 1 liter of $K_2Cr_2O_7$ 50 ppm). The mixture was then shaken in an orbital shaker for 1 hour at 150 rpm speed. After filtering, the solution was centrifuged using for 15 minutes at 150 rpm speed. The adsorption capacity (q) was counted with the equation:

$$\boldsymbol{q = \frac{(C_i - C_f)V_s}{m_a}} \quad (1)$$

Where q is the equilibrium adsorption capacity (mg adsorbate/g adsorbent), C_i is the initial concentration, C_f is the final concentration, V_s is the volume of the solution (liters), and m_a is the mass of the adsorbent (g) used (Kaushal & Singh, 2017).

p-ISSN: XXXX-XXXX
e-ISSN: XXXX-XXXX

3. RESULT AND DISCUSSION

PANI synthesis was carried out under acidic conditions using hydrochloric acid (HCl)(Fauziah et al., 2023). HCl was chosen because it is cheap and easy to obtain, effective in producing PANI with high purity and good stability. Using HCl allows the formation of PANI nanofibers with controllable diameters and can increase the electrical conductivity of the resulting PANI material (Zakaria et al., 2015). Ammonium persulfate (APS) was used as an oxidant because of its good solubility and ability to facilitate redox reactions in aqueous media (Herrera-Ordonez, 2022). The synthesis results showed that all samples had an almost uniform green color, a PANI ES characteristic (Fauziah et al., 2023).

3.1 The effect of APS concentration variation

The difference in APS concentration affected the amount of PANI mass formed, as seen in Figure 2. APS concentration of 0.1 M produced 0.38 g of PANI, APS 0.3 M (1.19 g), APS 0.5 M (2.34 g) and APS 0.7 M (3.03 g). Increasing the concentration from 0.1 to 0.7 M increased the amount of reaction product almost 10 times. This increase in mass is due to the increase in APS concentration, increasing the chemical energy in the reaction system, producing more reaction points, and accelerating the polymerization rate (Qiu et al., 2020). Increasing the APS concentration accelerates the production of PANI by increasing the number of free radicals that initiate the aniline polymerization process. The more persulfate radicals formed, the more aniline radicals formed (Yang & Chen, 1995), accelerating the reaction and increasing the total amount of PANI formed. The amount of APS used in the reaction will affect the resulting branching (Ketut Umiati & Azam, 2024), which causes an increase in the amount of PANI produced.

p-ISSN: XXXX-XXXX
e-ISSN: XXXX-XXXX

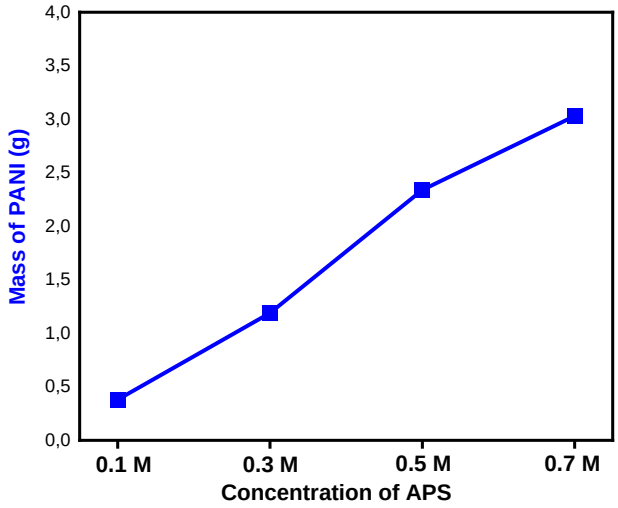

Figure 2. The plot of the mass of PANI produced against the concentration of APS using.

3.2 The FTIR spectrum of PANI

The FTIR spectrum of aniline monomer in Figure 3a shows the presence of peaks at wave numbers 3356 cm^{-1} and 3424 cm^{-1}, indicating the presence of N–H stretching modes (primary amines). The disappearance of these peaks confirms the successful formation of polyaniline from aniline. The presence of typical PANI peaks, such as C=C stretching in the quinonoid ring (Q) (1560 cm^{-1}) and C=C in the benzenoid ring (B) (1475 cm^{-1}), also confirms that PANI has been formed (Fauziah et al., 2023). The other confirmation is given with the presence of the C – N stretching in the quinonoid ring (1301 cm^{-1}), the C~$N^{+\cdot}$ protonation stretching vibration in the polaronic structure (1244 cm^{-1}), the aromatic C–H plane (1139 cm^{-1}), and the amine stretching vibration (1182 cm^{-1}) (Kamarudin et al., 2021). The FTIR spectrum also shows a long tail-like shape at wave numbers above 2000 cm^{-1}, which indicates the resulting PANI form as PANI ES. The PANI ES form is also supported by the presence of C=C stretching intensity in the quinonoid ring (Q) and C=C in the benzenoid ring (B), which are almost the same (Fauziah et al., 2023).

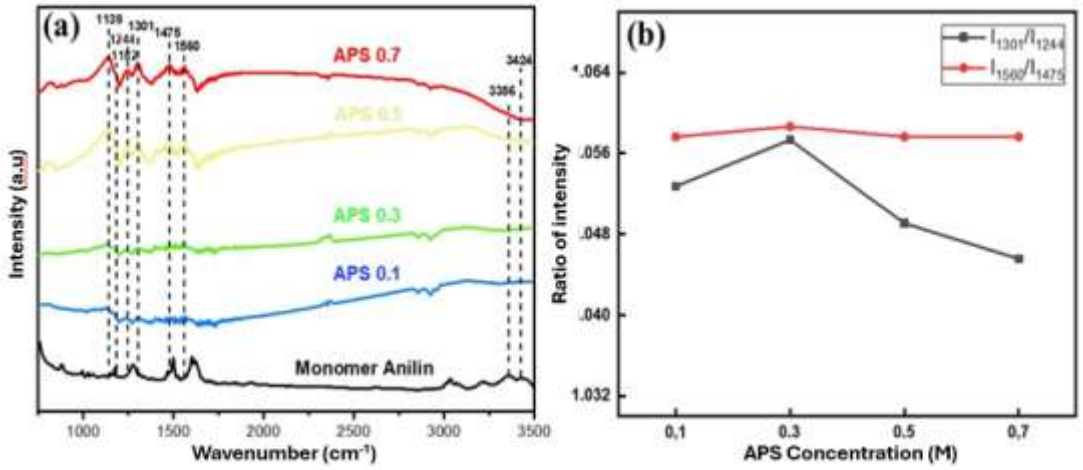

Figure 3. The plot of (a) FTIR spectrum of PANI with APS concentrations of 0.1, 0.3, 0.5, 0.7 M and aniline monomer (b) the ratio of characteristic peak intensities.

The comparison of the peak intensity of the quinonoid peak to the benzenoid peak is expressed as I_{1560}/I_{1475}. The I_{1560}/I_{1475} value in Figure 3 (b) is not significantly different from the value in the range of 1. It indicates that all PANI samples with various concentrations have the Emeraldine Salt form (Kamarudin et al., 2021). The PANI ES form prediction can use the peak intensity ratio of 1301 to 1244. The I_{1301}/I_{1244} value indicates the relative number of polarons along the PANI chain (Fauziah et al., 2023). Figure 3b shows that PANI synthesized with an APS concentration of 0.3 M has more polarons than PANI with other APS concentration variations. It shows that PANI with an APS concentration variation of 0.3 M has a PANI ES form compared to the others.

3.3 The Raman spectrum of PANI

Figure 4a shows the Raman spectrum of all samples of PANI. The peak at 1593 cm^{-1} for the C=C stretching of the benzenoid ring and the peak at 1489 cm^{-1} for the C=C stretching of the quinonoid ring (Pasela et al., 2019). The ratio of the quinonoid ring's intensity to the benzonoid's intensity is an I_{1489}/I_{1593} value. The I_{1489}/I_{1593} values of all PANI shown in Figure 4.b show that all APS concentrations have a similar intensity ratio, indicating that all PANI are in the emeraldine form (Fauziah et al., 2023). This data aligns with the data taken from the FTIR data. The bending vibration of the C – H plane on the benzenoid ring at 1193 cm^{-1} and the C–H bending on the quinonoid bend at 1166 cm^{-1} (Fauziah et al., 2023). The data show that the variation of the concentration of APS added does not affect the oxidation level; the entire PANI is in the form of PANI ES. The variation of APS added affects the mass of the resulting polyaniline. The identification of polaron changes using a peak at 1341 cm^{-1} for the presence of $C{\sim}N^{+\cdot}$ stretching and a peak at 1212 cm^{-1} for C–N stretching (C. Gomes & A. S. Oliveira, 2012). If the peak intensity at 1212 cm^{-1} decreases while the peak intensity at 1341 cm^{-1} increases, C–N has

p-ISSN: XXXX-XXXX
e-ISSN: XXXX-XXXX

become the polaron form. When the peak ratio intensity of 1341 to 1212 increases, more polaron species are indicated in PANI (Fauziah et al., 2023). The enhanced polaron formation may contribute to higher adsorption efficiency. PANI with APS 0.7 M has I_{1341}/I_{1212} higher than PANI with APS 0.5 M. PANI APS 0.7 M is a better adsorbent candidate compared to PANI with APS 0.5 M. PANI with APS 0.3 M has I_{1341}/I_{1212} have almost the same value with PANI APS 0.7 M, due to the PANI APS 0.7 M give highest yield. PANI APS 0.7 M becomes the best candidate for adsorbent agents.

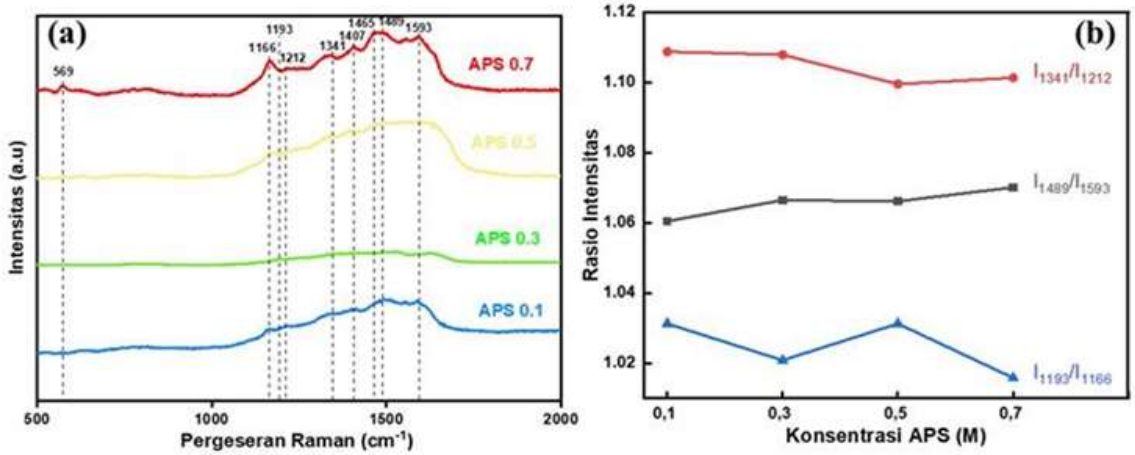

Figure 4. The plot of (a) Raman spectrum of PANI with APS concentrations of 0.1, 0.3, 0.5, and 0.7 M (b the intensity ratio of several peaks with varying concentrations.

3.4 The adsoption Capacity of PANI

Preliminary tests conducted on all samples using 50 ppm $K_2Cr_2O_7$ solution (Figure 5a) showed almost the same adsorption power, as seen in Figure 5b. The analysis showed that the adsorption of Cr (VI) metal using PANI material gave good results at all concentration variations. PANI synthesized with APS and HCl doping could remove Cr (VI) metal in water (Samani et al., 2010). The Cr (VI) solution before adsorption was bright yellow, while after adsorption with the PANI sample, the solution turned colorless, indicating that the PANI sample successfully adsorbed Cr (VI) metal in water very well. The adsorption power is almost the same for all samples, while the highest yield is when an APS concentration of 0.7 M; then, the best candidate for adsorbent obtained from the results of concentration variations is PANI with an APS concentration of 0.7 M. Further analysis on PANI produced with an APS variation of 0.7 M using AAS of the adsorption power of PANI APS 0.7 M showed a value of 14.22 mg/g. This process involves electron transfer between PANI and Cr(VI), increasing adsorption power. The amine group ($-NH_2$) in polyaniline can interact strongly with Cr (VI) through electrostatic interactions or the formation of hydrogen bonds or direct coordination with metal ions, increasing the adsorption capacity (Samani et al., 2010). The size of the PANI also supports this factor, which was produced based on the SEM image analysis. PANI synthesized with 0.7 M APS has a globular shape

measuring 75 - 106 nm (Figure 5c). The PANI with a 10.2 pore size has a better adsorption capacity with the range of 43.6 to 233.7 mg/g due to the PANI confining in the pores of polystyrene beads(Ding et al., 2018).

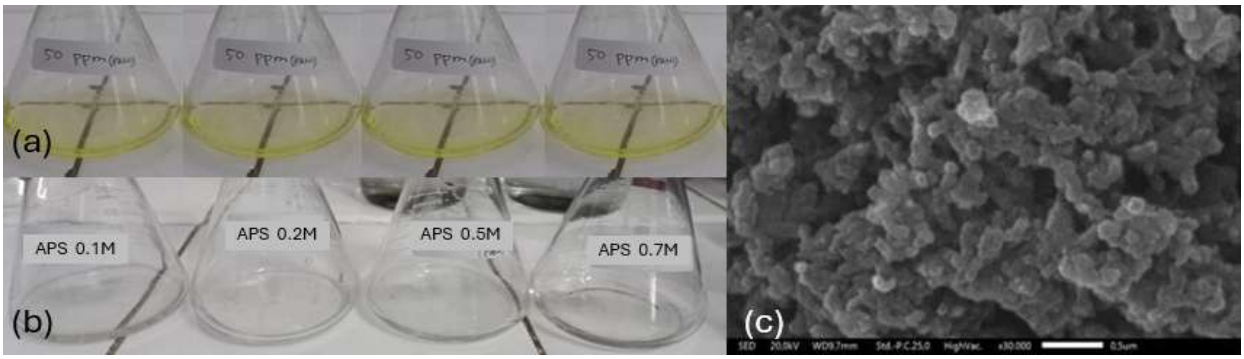

Figure 5. The image of 50 ppm Chromium solution (a) before adsorption, (b) after adsorption, and (c) the SEM image of PANI with APS 0.7 M concentration.

4. CONCLUSIONS

The study of APS concentration variation in polyaniline synthesis shows that concentration variation does not affect the oxidation level of polyaniline produced, but all polyaniline is in ES form. The APS concentration variation only affects the yield of polyaniline produced. This research indicates that PANI synthesis by the rapid mixing method at an APS concentration of 0.7 M is an efficient synthesis method to obtain nano-sized PANI material with good adsorption capacity for chromium (VI) metal ions. This research is still limited to a laboratory scale and has not tested on absolute waste; it must apply to real waste. Further research is needed to test the effectiveness of this adsorbent in a continuous system and field conditions. Using the other oxidation level of PANI or the emeraldine base of PANI as an adsorbent may give higher adsorption capacity.

ACKNOWLEDGMENTS

N. Fauziah acknowledges Prof. Veinardi Suendo for facilitating the FTIR and Raman measurement, and also acknowledge for the assistance and support from the leaders and all the Mathematics and Science Faculty of Universitas Garut (UNIGA).

BIBLIOGRAPHY

Amalina, A. N., Suendo, V., Reza, M., Milana, P., Sunarya, R. R., Adhika, D. R., & Tanuwijaya, V. V. (2019). Preparation of Polyaniline Emeraldine Salt for Conducting-Polymer-Activated Counter Electrode in Dye Sensitized Solar Cell (DSSC) using Rapid-Mixing Polymerization at Various Temperature. *Bulletin of Chemical Reaction Engineering &Amp; Catalysis*, *14*(3), 521. https://doi.org/10.9767/bcrec.14.3.3854.521-528

C. Gomes, E., & A. S. Oliveira, M. (2012). Chemical Polymerization of Aniline in Hydrochloric Acid (HCl) and Formic Acid (HCOOH) Media. Differences Between the Two Synthesized Polyanilines. *American Journal of Polymer Science*, *2*(2), 5–13. https://doi.org/10.5923/j.ajps.20120202.02

Ding, J., Pu, L., Wang, Y., Wu, B., Yu, A., Zhang, X., Pan, B., Zhang, Q., & Gao, G. (2018). Adsorption

and Reduction of Cr(VI) Together with Cr(III) Sequestration by Polyaniline Confined in Pores of Polystyrene Beads. *Environmental Science and Technology*, *52*(21), 12602–12611. https://doi.org/10.1021/acs.est.8b02566

Eskandari, E., Kosari, M., Davood Abadi Farahani, M. H., Khiavi, N. D., Saeedikhani, M., Katal, R., & Zarinejad, M. (2020). A Review on Polyaniline-Based Materials Applications in Heavy Metals Removal and Catalytic Processes. *Separation and Purification Technology*, *231*(August 2019). https://doi.org/10.1016/j.seppur.2019.115901

Fauziah, N., Khasannah, W. L., Andari, G. A., Fatya, A. I., Benu, D. P., Steky, F. V., Milana, P., Hidayat, R., & Suendo, V. (2023). Eco-friendly Direct-current Pulsed Electropolymerization of Polyaniline Nanofibers on Synthetic Graphite Substrate for Counter Electrode in Dye-Sensitized Solar Cells. *Polymer-Plastics Technology and Materials*, *62*(6), 800–815. https://doi.org/10.1080/25740881.2022.2151064

Georgaki, M. N., & Charalambous, M. (2023). Toxic Chromium in Water and the Effects on the Human Body: a Systematic Review. *Journal of Water and Health*, *21*(2), 205–223. https://doi.org/10.2166/wh.2022.214

Goswami, S., Nandy, S., Fortunato, E., & Martins, R. (2023). Polyaniline and its Composites Engineering: a Class of Multifunctional Smart Energy Materials. *Journal of Solid State Chemistry*, *317*(October 2022), 123679. https://doi.org/10.1016/j.jssc.2022.123679

Hashem, M. A., Mim, M. W., Noshin, N., & Maoya, M. (2024). Chromium Adsorption Capacity from Tannery Wastewater on Thermally Activated Adsorbent Derived from Kitchen Waste Biomass. *Cleaner Water*, *1*(December 2023), 100001. https://doi.org/10.1016/j.clwat.2023.100001

Herrera-Ordonez, J. (2022). The Role of Sulfate Radicals and pH in the Decomposition of Persulfate in Aqueous Medium: A Step Towards Prediction. *Chemical Engineering Journal Advances*, *11*(May), 100331. https://doi.org/10.1016/j.ceja.2022.100331

Kamarudin, S., Rani, M. S. A., Mohammad, M., Mohammed, N. H., Su'ait, M. S., Ibrahim, M. A., Asim, N., & Razali, H. (2021). Investigation on Size and Conductivity of Polyaniline Nanofiber Synthesised by Surfactant-free Polymerization. *Journal of Materials Research and Technology*, *14*, 255–261. https://doi.org/10.1016/j.jmrt.2021.06.057

Kaushal, A., & Singh, S. K. (2017). Critical Analysis of Adsorption Data Statistically. *Applied Water Science*, *7*(6), 3191–3196. https://doi.org/10.1007/s13201-016-0466-4

Kusumatmadja, S., (1995) Keputusan Menteri Negara Lingkungan Hidup. *KEP-51/MENLH/10/1995 tentang Baku Mutu Limbah Cair bagi Kegiatan Industri*.

Ketut Umiati, N. A., & Azam, M. (2024). Effect of Ammonium Peroxydisulphate (APS) Addition on Polyaniline Nanofiber Microstructure in Interfacial Polymerization Method. *International Journal of Research and Review*, *11*(6), 517–523. https://doi.org/10.52403/ijrr.20240657

Liang, H., Zhang, H., Zhao, P., Zhao, X., Sun, H., Geng, Z., & She, D. (2021). Synthesis of A Novel Three-dimensional Porous Carbon Material and its Highly Selective Cr(VI) Removal in Wastewater. *Journal of Cleaner Production*, *306*, 127204. https://doi.org/10.1016/j.jclepro.2021.127204

Nurianingsih, R., Sriatun, S., & Darmawan, A. (2019). Polyaniline Modified Natural Zeolite as Adsorbent for Chromium(III) Metal Ion. *Jurnal Kimia Sains Dan Aplikasi*, *22*(6), 292–298. https://doi.org/10.14710/jksa.22.6.292-298

Palimkar, S., Galgali, P., Jape, A. A., Singh, S. K., Adhikari, A., Patel, R., & Routh, J. (2023). Critical Assessment of Polyaniline-based Biocomposites for Removal of Toxic Heavy Metals from Aqueous Media. *Asian Journal of Chemistry*, *35*(7). https://doi.org/10.14233/ajchem.2023.27945

Pasela, B. R., Castillo, A. P., Simon, R., Pulido, M. T., Mana-ay, H., Abiquibil, M. R., Montecillo, R., Thumanu, K., Tumacder, D. von, & Taaca, K. L. (2019). Synthesis and Characterization of Acetic acid-doped Polyaniline and Polyaniline-chitosan Composite. *Biomimetics*, *4*(1). https://doi.org/10.3390/biomimetics4010015

Qiu, B., Wang, J., Li, Z., Wang, X., & Li, X. (2020). Influence of Acidity and Oxidant Concentration on

the Nanostructures and Electrochemical Performance of Polyaniline During Fast Microwave-assisted Chemical Polymerization. *Polymers*, *12*(2). https://doi.org/10.3390/polym12020310

Reza, M., Srikandi, N., Amalina, A. N., Benu, D. P., Steky, F. V., Rochliadi, A., & Suendo, V. (2019). Variation of Ammonium Persulfate Concentration Determines Particle Morphology and Electrical Conductivity in HCl Doped Polyaniline. *IOP Conference Series: Materials Science and Engineering*, *599*(1). https://doi.org/10.1088/1757-899X/599/1/012002

Reza, M., Utami, A. N., Amalina, A. N., Benu, D. P., Fatya, A. I., Agusta, M. K., Yuliarto, B., Kaneti, Y. V., Ide, Y., Yamauchi, Y., & Suendo, V. (2021). Significant Role of Thorny Surface Morphology of Polyaniline on Adsorption of Triiodide Ions Towards Counter Electrode in Dye-Sensitized Solar Cells. *New Journal of Chemistry*, *45*(13), 5958–5970. https://doi.org/10.1039/d0nj06180h

Samani, M. R., Borghei, S. M., Olad, A., & Chaichi, M. J. (2010). Removal of Chromium from Aqueous Solution using Polyaniline - Poly ethylene glycol composite. *Journal of Hazardous Materials*, *184*(1–3), 248–254. https://doi.org/10.1016/j.jhazmat.2010.08.029

Senania, A. and N. (2022). Analisis Parameter Air Limbah Industri Penyamakan Kulit Sukaregang Garut. *Lantanida Journal*, *10*(1), 1–9. https://jurnal.ar-raniry.ac.id/index.php/lantanida/article/view/11088

Stejskal, J., Kratochvíl, P., & Jenkins, A. D. (1996). The Formation of Polyaniline and the Nature of its Structures. *Polymer*, *37*(2), 367–369. https://doi.org/10.1016/0032-3861(96)81113-X

Sunarya, R. R., Hidayat, R., Radiman, C. L., & Suendo, V. (2020). Electrocatalytic Activation of a DSSC Graphite Composite Counter Electrode Using In Situ Polymerization of Aniline in a Water/Ethanol Dispersion of Reduced Graphene Oxide. *Journal of Electronic Materials*, *49*(5), 3182–3190. https://doi.org/10.1007/s11664-020-07977-3

Wang, L., Shi, C., Pan, L., Zhang, X., & Zou, J. J. (2020). Rational Design, Synthesis, Adsorption Principles and Applications of Metal Oxide Adsorbents: A review. *Nanoscale*, *12*(8), 4790–4815. https://doi.org/10.1039/c9nr09274a

Xie, S. (2024). Water Contamination Due to Hexavalent Chromium and its Health Impacts: Exploring Green Technology for Cr (VI) Remediation. *Green Chemistry Letters and Reviews*, *17*(1), 1–19. https://doi.org/10.1080/17518253.2024.2356614

Yang, S. M., & Chen, J. T. (1995). The Effect of Synthesis Conditions on the Properties of Polyaniline Film. *Synthetic Metals*, *69*(1–3), 153–154. https://doi.org/10.1016/0379-6779(94)02399-J

Zakaria, Z., Halim, N. F. A., Schleusingen, M. H. V., Islam, A. K. M. S., Hashim, U., & Ahmad, M. N. (2015). Effect of Hydrochloric Acid Concentration on Morphology of Polyaniline Nanofibers Synthesized by Rapid Mixing Polymerization. *Journal of Nanomaterials*, *2015*. https://doi.org/10.1155/2015/218204